Activation of DDX58/RIG-I suppresses the growth of tumor cells by inhibiting STAT3/CSE signaling in colon cancer

YUYING DENG, HAN FU, XUE HAN, YUXI LI, WEI ZHAO, XUENING ZHAO, CHUNXUE YU, WENQING GUO, KAIJIAN LEI and TIANXIAO WANG

Biopharmaceutical Department, School of Pharmacy, Henan University, Kaifeng, Henan 475004, P.R. China

Received March 28, 2022; Accepted July 12, 2022

DOI: 10.3892/ijo.2022.5410

Abstract. Some patients with colon cancer eventually develop metastasis during treatment, and the 5-year survival rate of patients with metastatic colon cancer remains relatively low, which is most likely due to the ineffectiveness of the current standard treatment. Systemic treatment for patients with colon cancer has expanded from chemotherapy to targeted therapy and immunotherapy. Immunotherapy holds promise in the treatment of colon cancer. The present study revealed the role of innate immune receptor helicase DExD/H-box helicase 58 (DDX58), which encodes retinoic acid-inducible gene-I (RIG-I), in colon cancer. It was demonstrated that colon cancer patients with a low protein expression of DDX58/RIG-I had a worse 5-year survival rate of patients compared with patients with a high expression of DDX58/RIG-I. The activation of DDX58/RIG-I inhibited the proliferation, migration and invasion of colon cancer cells, as well as tumor growth in a nude mouse xenograft model of colon cancer. To investigate the mechanisms of action of DDX58/RIG-I in colon cancer, the role of signal transducer and activator of transcription 3 (STAT3)/cystathionine-γ-lyase (CSE) signaling in the up- or downregulation of DDX58 was examined. The data demonstrated that DDX58 regulated the STAT3/CSE signaling pathway by interacting with STAT3 and consequently affecting the proliferation of tumor cells in colon cancer. In addition, the RIG-I agonist, SB9200, induced proliferation, migration and invasion of human colon cancer. On the whole, the present study demonstrates that DDX58/RIG-I affects the proliferation of tumor cells by regulating STAT3/CSE signaling in colon cancer. The findings presented herein suggest that DDX58/RIG-I activation may be an effective treatment strategy, and DDX58/RIG-I agonists may be potential therapeutic candidates for colon cancer.

Correspondence to: Professor Kaijian Lei or Professor Tianxiao Wang, Biopharmaceutical Department, School of Pharmacy, Henan University, North part of Jinming Road, Kaifeng, Henan 475004, P.R. China
E-mail: leikaijian@126.com
E-mail: wtx1975@126.com

Key words: DExD/H-box helicase 58, retinoic acid-inducible gene-I, signal transducer and activator of transcription 3, cystathionine-γ-lyase, colon cancer

Introduction

Colon cancer is the third most prevalent type of cancer worldwide. Systemic treatment for patients with colon cancer has expanded from chemotherapy to targeted therapy and immunotherapy. Therefore, it is critical to explore new biomarkers for the systematic treatment of colon cancer including targeted therapy and immunotherapy.

DExD/H-Box Helicase 58 (DDX58) encodes retinoic acid-inducible gene-I (RIG-I), which is an innate immune receptor helicase (1-3). RIG-I is widely expressed in a variety of tissues and cells and is involved in the production of interferons to initiate innate antiviral immunity (4-6). However, it has been indicated that RIG-I also participates in cancer cellular activities. For example, the activation of RIG-I signaling triggers apoptotic programs in tumor cells and activates antitumor immunity (7,8). In hepatocellular carcinoma, a low RIG-I expression is associated with a poor survival; that is, RIG-I functions as a tumor suppressor by enhancing signal transducer and activator of transcription (STAT)1 activation by competitively binding the SH2 domain of STAT1 against its negative regulator SHP1 (9,10). In breast cancer, RIG-I activation decreases tumor growth and metastasis (11,12). Additionally, DDX58/RIG-I expression can also affect immune response-based cancers, and $CD4^+$ and $CD8^+$ T-cells and T-cell-mediated effects enhance the antitumor efficacy of RIG-I agonists (13). The inhibition of the MAPK pathway mediates inflammatory reprogramming and renders tumors sensitive to the targeted activation of RIG-I, while a high MAPK activation has been shown to be associated with the reduced presence of $CD8^+$ T-cells (14). Overall, these findings suggest that RIG-I plays more diverse roles in a variety of cellular activities, and its function goes far beyond that of a pattern recognition receptor. Therefore, on the basis that RIG-I exhibits tumor-suppressive activity, the successful therapeutic delivery of RIG-I agonists could induce tumor cell apoptosis and modulate the tumor microenvironment.

To the best of our knowledge, there are no data available to date on the clinical significance of RIG-I in colon cancer. Therefore, the present study aimed to investigate the value of RIG-I in colon cancer to address the urgent need to improve

the management of this tumor type. The second aim was to identify the factors associated with RIG-I expression to characterize the RIG-I-associated microenvironment and the immunotherapeutic options of colon cancer.

In the present study, *in vivo* and *in vitro* experiments were performed to explore the value and signature of DDX58/RIG-I in colon cancer. It was found that a low DDX58/RIG-I expression was associated with an increase in the proliferation, migration and invasion of colon cancer cells. In addition, the activation of DDX58/RIG-I suppressed the proliferation of tumor cells by inhibiting STAT3/cystathionine-γ-lyase (CSE) signaling in colon cancer. These findings suggest that the activation of DDX58/RIG-I may be an effective treatment strategy for colon cancer.

Materials and methods

Cell lines and animals. HCT8 and HCT116 human colon cancer cell lines and FHC human normal colorectal mucosal cells were generously donated by the Army Medical University (Chongqing, China). SW620 and LOVO human colon cancer cell lines were generously donated by Tongji University (Shanghai, China). SW480 human colon cancer cells were generously donated by the School of Basic Medicine, Henan University (Kaifeng, China). The cell lines (HCT116, CCL-247; HCT8, CCL-244; LOVO, CCL-229; SW480, CCL-228; SW620, CCL-227; FHC, CRL-1831) were purchased on the ATCC platform. Cell lines were tested using short tandem repeat (STR) analysis as follows: DNA was extracted and the STRs were amplified by multiplex PCR and separated on a genetic analyzer. The signals were then analyzed using GeneMapper software v4.1 (Applied Biosystems; Thermo Fisher Scientific, Inc.). The colon cancer cells, HCT8, SW480 and LOVO, were used in RPMI-1640 medium (Thermo Fisher Scientific, Inc.), the SW620 cells in Dulbecco's modified Eagle's medium (Thermo Fisher Scientific, Inc.), the HCT116 cells in McCoy's 5A medium (Biological Industries) and the FHC cells in DMEM/F-12 (Beijing Solarbio Science & Technology Co., Ltd.). All cells were cultured in a humidified atmosphere of 5% CO_2 at 37˚C.

Balb/c nude mice (n=12; specific pathogen-free; male; age, 4-5 weeks) weighing 18-22 g were supplied by Beijing Viton Lihua Experimental Animal Technology [certificate no. SCXK (Jing) 2016-0006, no. 110011210107417128; Beijing, China]. The mice were allowed free access to food and water and were housed in an environment with a constant temperature and humidity (temperature, 24±1˚C; humidity, 50-70%), ventilation rate (10-20 times/h), noise (<40 db) and working illumination (250 lx) under a 12-h light/dark cycle. The drinking water, food, and experimental supplies were sterilized and disinfected. The present study was approved by the Ethics Committee of the Medical School of Henan University (HUSOM2020-301).

Tissue microarray analysis. A human colon cancer microarray (HColA180Su13) containing 90 tumor samples and 90 para-carcinoma samples was constructed by Shanghai Outdo Biotech Co., Ltd. The clinicopathological characteristics of the tumor samples are presented in Table I. Each tissue was stained with anti-DDX58 antibody (diluted in PBS; cat. no. 20566-1-AP, supplier: ProteinTech Group, Inc.) as the primary antibody (4˚C, 16 h) and the secondary antibody (C2 biotin-labeled sheep anti-mouse/rabbit IgG polymer, cat. no. KIT-9707, Fuzhou Maixin Biotech. Co., Ltd.) was incubated at room temperature for 45 min with UltraSensitive SP reagent box (Maixin Inc.) Automatic immunohistochemical staining was accomplished using Autostainer Link 48 (Dako; Agilent Technologies, Inc.) The integral intensity value was measured with Aperio ImageScope software v12.4.3 (Aperio, Leica GmbH). All experiments were performed in accordance with national ethical guidelines and with the approval from all patients and the committee of Shanghai Outdo Biotech Co., Ltd.

The immunohistochemistry test score criteria were as follows: i) Determination of the staining intensity: The whole field of tissue points was observed under low magnification (x40 and x200) and the tissues were classified into weak positive, medium positive and strong positive. Weak positive was light yellow (+ or 1), medium positive was brownish yellow (++ or 2) and strong positive was tan (+++ or 3). ii) Determination of the staining positive rate: Firstly, tissue points were observed in the whole field under a low-power lens of Aperio XT (Leica GmbH), and then three fields with different staining intensity were selected for interpretation under a high-power lens of AperioXT (Leica GmbH). If staining was located in cytoplasm, 100 cells were randomly recorded in each field, and the percentage of positive cells in 100 cells was then recorded x1%. In the same manner, the percentage of positive cells in the other two fields was x2% and x3%, and the average of the positive staining rate of this tissue point was obtained.

The data processing of human tissue chip was as follows: The total score was obtained by the product of staining score intensity and staining positive score, and the cut-off value was then determined according to the total score to determine the high, medium and low expression groups for survival. In the tissue microarray, a DDX58 staining score <1 was considered as a low protein expression, and a DDX58 staining score >1 and <1.5 was considered as a medium protein expression, and a DDX58 staining score ≥1.5 was considered as a high protein expression.

Construction of DDX58-overexpressing lentivirus. Full-length DDX58 cDNA (NM_014314) was cloned into the Ubi-MCS-SV40-EGFP-IRES-puromycin vector (#63954-4; Shanghai GeneChem Co., Ltd.) to construct DDX58-overexpressing lentivirus. The DDX58-overexpressing lentivirus was used to infect the HCT8 and HCT116 cells to obtain stable cells overexpressing DDX58. Transfection was performed using HitransG P transfection reagent (Shanghai GeneChem Co., Ltd.), with a lentiviral titer of 4E+8 TU/ml and vector titer of 1E+9 TU/ml. The time between transfection and subsequent experiments was 2 weeks.

siRNA and plasmid transfection. For knockdown, HCT116/DDX58, HCT8/DDX58, HCT116, HCT8 and SW620 cells in six-well plates were transfected with scramble siRNA (Sc siRNA, 20 μM) or specific siRNA against human DDX58 (20 μM Invitrogen; Thermo Fisher Scientific, Inc.) or specific siRNA against human CSE (20 μM, Invitrogen; Thermo Fisher Scientific, Inc.) or specific siRNA against human STAT3

Table I. Clinicopathological characteristics of the tumor samples in the tissue microarray.

Characteristic	No. of patients
Age (years)	
≤60	32
>60	58
Sex	
Male	47
Female	43
Tumor grade	
I, II and I- II	76
I-III, II-III, III and III-IV	14
T stage	
T1/T2	11
T3/T4	79
N stage	
N0	61
N1/N2	29
M stage	
M0	87
M1	3
TNM stage	
I/II	59
III/IV	31
Tumor size (cm)	
≤5	12
>5	78

(20 μM, Invitrogen; Thermo Fisher Scientific, Inc.) using Lipofectamine 2000® (Invitrogen; Thermo Fisher Scientific, Inc.). The medium was replaced at 6 h post-transfection, and the silencing efficiency was determined using western blot analysis at 48 h post-transfection. The siRNA sequences were as follows: DDX58 siRNA sense, 5'-CCGGCACAGAAGUGUAUAUTT-3' and antisense, 5'-AUAUACACUUCUGUGCCGGTT-3'; CSE-specific siRNA sense, 5'-GGUUUAGCAGCCACUGUAAdTdT-3' and antisense, 5'-UUACAGUGGCUGCUAAACCdTdT-3'; STAT3-specific siRNA sense, 5'-CCCGUCAACAAAUUAAGAAdTdT-3' and antisense, 5'-UUCUUAAUUUGUUGACGGGdTdT-3'; Sc siRNA sense, 5'-UUCUCCGAACGUGUCACGUTT-3' and antisense, 5'-ACGUGACACGUUCGGAGAATT-3.

In addition, for SW620 cells, DDX58 overexpression plasmid (GV367-vector and GV367-hDDX58, Shanghai GeneChem Co., Ltd.) was used for transfection, for the HCT116, HCT8, SW620 cells, STAT3 overexpression plasmid transfection was performed as follows: pCMV-FLAG vector and pCMV-FLAG-hSTAT3 were provided as a gift from Military Medical Sciences School. The plasmids (600 ng/μl) were transiently transfected using Lipofectamine 2000® reagent (Invitrogen; Thermo Fisher Scientific, Inc.) according to the manufacturer's instructions. After 6 h, the cells were exposed to fresh medium.

Cell viability and proliferation assays. The cells (HCT8, HCT116 and SW620) were seeded into 96-well plates at a density of $1x10^4$ cells per well for 48 h. Cell viability was evaluated by determining the number of cells using MTS (MilliporeSigma) assay, and after 4 h, the absorbance was measured at 570 nm by enzyme-labeled instrument (PerkinElmer; Thermo Fisher Scientific, Inc.). For cell proliferation assay, the HCT8, HCT116 and SW620 cells ($1x10^5$/ml, 100 μl/well) were seeded in 96-well plates, and cell proliferation was assessed according to the number of EdU^+ cells using an EdU assay kit (Guangzhou RiboBio Co., Ltd.) that included the processing of EdU markers, cell fixation, Apollo staining and DNA staining with the Hoechst 33342 reaction. Each experiment was performed in triplicate and repeated three times. A microcope was used (U-LH100HG; Olympus Corporation) to obtain images. ImageView (version 3.7) software was used for processing analysis.

Scratch wound assay. The cell scratch wound assay is an *in vitro* method used to examine cell migration (15). For this assay, the cells were grown to 90% confluency in a six-well plate. A 10-μl pipette tip was used to scratch a straight wound in cells in 35-mm dishes. The detached cells were removed by washing with phosphate-buffered saline (PBS), and serum-free medium was used to continue cell culture. After using a digital camera (EOS450-D; China Canon Co. Ltd.) and scraping at 0, 24 or 48 h, migration images were obtained and the gap closing rates were compared. Adobe Photoshop CC software was used for analysis.

Transwell assay. Transwell assays were performed to investigate cell migration and invasion in 24-well Transwell chambers (pore size, 8 μm; Corning, Corning, Inc.). The Transwell chambers were covered with or without Matrigel matrix (BD Biosciences) for invasion or migration assays, respectively. The cells ($1x10^5$ cells/ml) were suspended in serum-free medium and inoculated in the upper chamber, and medium containing 10% FBS was added to the lower chamber. Following incubation for 24 h at 37˚C, the cells were fixed at room temperature with 4% cell fixative (Beijing Solarbio Science & Technology Co., Ltd.) for 30 min and stained with 0.1% crystal violet (Beijing Solarbio Science & Technology Co., Ltd) for 15 min, then washed with water, dried and photographed as previously described (16-18).

Western blot analysis. The cells or tissues were washed with ice-cold PBS and lysed for 20 min on ice using RIPA lysis buffer (ProteinTech Group, Inc.) with both protease and phosphatase inhibitors. Protein concentrations were determined using a BCA protein assay kit (Beijing Solarbio Science & Technology Co., Ltd.), and western blot analysis was then performed using a standard protocol. A total of 30 μg of protein was separated by 8% SDS-PAGE and transferred to a polyvinylidene difluoride membrane (MilliporeSigma) at 70 mA for 2 h. The membrane was then blocked in 5% fat-free milk, and probed with specific primary antibodies against DDX58, STAT3, p-STATS and CSE at 4˚C overnight. Following incubation with the secondary antibody, the proteins were visualized using an K ECL Enhanced Chemiluminescence kit (Kemix, Ltd.) and detected using a FluorChem Q Multifluor

System (ProteinSimple). Densitometric analysis was performed using Image J 1.51j8 software (National Institutes of Health). The antibodies used were as follows: DDX58 rabbit polyclonal antibody (1:1,000, cat. no. 20566-1-AP, ProteinTech Group, Inc.), STAT3 mouse monoclonal antibody (1:1,000, cat. no. 9139S, Cell Signaling Technology, Inc.), p-STAT3 rabbit polyclonal antibody (1:1,000, cat. no. 9131S, Cell Signaling Technology, Inc.), CSE rabbit polyclonal antibody (1:3,000, cat. no. F052208, Abways Technology) and GAPDH mouse monoclonal antibody (1:100,000, cat. no. 60004-1-lg, ProteinTech Group, Inc.), HRP-goat anti-rabbit IgG (1:3,000, cat. no. SA00001-2, ProteinTech Group, Inc.), HRP-goat anti-mouse IgG (1:3,000, cat. no. SA00001-1, ProteinTech Group, Inc.)

Reverse transcription-quantitative PCR (RT-qPCR). Total RNA was extracted from the cells using TRIzol reagent (Ambion; Thermo Fisher Scientific, Inc.) and reverse transcribed with HiScript II Q RT SuperMix for qPCR (Vazyme Biotech Co., Ltd.) in accordance with a standard protocol (50˚C, 15 min; 85˚C, 5 sec). qPCR was performed on a SLAN-96S Real-Time PCR System (Shanghai Hongshi Medical Technology Co., Ltd.) using hamQ Universal SYBR qPCR Master Mix (Vazyme Biotech Co., Ltd.). The PCR conditions were as follows: 30 sec at 95˚C pre-denaturation; 5 sec at 95˚C for denaturation, 30 sec at 60˚C for annealing and extension, a total of 40 cycles. The $2^{-\Delta\Delta Cq}$ method was used to evaluate the mRNA expression levels of genes. Please refer to the literature for specific method (19). The following primers were used in the RT-qPCR assay: DDX58 forward, 5'-AGAGCACTTGTGGACGCTTT-3' and DDX58 reverse, 5'-AGCAACTGAGGTGGCAATCA-3'; and GAPDH forward, 5'-GCACCGTCAAGGCTGAGAAC-3' and GAPDH reverse, 5'-TGGTGAAGACGCCAGTGGA-3'.

Co-immunoprecipitation (Co-IP) assay. A total of $3x10^7$ HCT116 cells were treated with NP-40 lysis buffer (Beijing Solarbio Science & Technology Co., Ltd.) and lysates were then incubated with DDX58 antibody-conjugate and protein A+G Agarose (Beyotime Institute of Biotechnology) overnight at 4˚C. Beads containing affinity-bound proteins were washed three times with PBS buffer, followed by elution with 1 ml NP-40 lysis buffer (Beijing Solarbio Science & Technology Co., Ltd.) three times. All tubes were centrifuged at 4˚C at 1,500 x g for 5 min, the supernatant was discarded, 1 ml cold PBS was added for washing; the tubes were centrifuged again at 1,500 x g for 1 min, and this was repeated three times; the beads were then cleaned with NP-40 lysis solution three times. The method was the same as that used for PBS washing. Finally, the supernatant liquid was discarded, followed by the addition of 40 μl 2X sample (Beijing Solarbio Science & Technology Co., Ltd.) to the IP group, 25 μl 2X sample (Beijing Solarbio Science & Technology Co., Ltd.) to the IgG group, and 5X sample (Beijing Solarbio Science & Technology Co., Ltd.) to the Input group, and then placed in a dry bath incubator (Hangzhou Aosheng Instruments Co., Ltd.) for 8 min. Following denaturation, proteins were separated on sodium dodecyl sulfate-polyacrylamide gels and transferred onto polyvinylidene difluoride membranes (MilliporeSigma) The membranes were probed with anti-DDX58 (Protein Tech Group, Inc.) or anti-STAT3 (Cell Signaling Technology, Inc.) antibodies. In this part, western blot analysis was used to detect the expression level of the target band. Primary antibody was incubated at 4˚C, 11 rpm for 14 h. Secondary antibody was incubated at 37˚C, 60 rpm for 2 h. The antibodies used were as follows: DDX58 rabbit polyclonal antibody (1:1,000, cat. no. 20566-1-AP, ProteinTech Group, Inc.), STAT3 mouse monoclonal antibody (1:1,000, cat. no. 9139S, Cell Signaling Technology, Inc.). HRP-Goat Anti-Rabbit IgG (1:3,000, cat. no. SA00001-2, ProteinTech Group, Inc.). HRP-Goat Anti-Mouse IgG (1:3,000, cat. no. SA00001-1, ProteinTech Group, Inc.).

Animal experiments. Animal experiments were approved by the Ethics Committee of Medical School of Henan University (HUSOM2020-301). BALB/c nude mice were injected subcutaneously into their right flanks with $3x10^6$ HCT116 cells infected with empty vector lentivirus or DDX58-overexpressing lentivirus. After 3 weeks, the experimental animals were first anesthetized (10% chloral hydrate, 400 mg/kg, administered via intraperitoneal injection). The mice were then sacrificed by cervical dislocation, resulting in immediate death. The death of the experimental animals was confirmed by the cessation of respiration, heartbeat, and pupil and nerve reflex. The tumors were then harvested, weighed and lysed using RIPA buffer for use in western blot analysis to detect the levels of DDX58, STAT3, pSTAT3 and CSE, as described above.

SB9200. SB9200 was obtained from MedChemExpress (inarigivir soproxil, cat. no. HY-109035). The HCT116 and SW620 cells were treated with SB9200 at a concentration of 80 μM. Cell viability was detected using MTS assay. Cell proliferation was detected using EdU assay. Wound healing was used to detect cell migration. Cell migration and invasion was examined using Transwell assay (all as described above).

Statistical analysis. Each experiment was repeated at least three times and graphs were created using GraphPad Prism software 6.0 (GraphPad Software Inc.). Statistical analyses were performed using SPSS 17.0 software (SPSS, Inc.). Data are expressed as the mean ± standard deviation. Differences between multiple groups were analyzed using one-way analysis of variance followed by Tukey's multiple comparisons test. $P<0.05$ was considered to indicate a statistically significant difference. The matched sample data in Fig. 1B were compared using a paired t-test and the data in Fig. 2D were compared used an unpaired t-test. The Kaplan-Meier method was used for survival analysis, and the log-rank was used to determine the differences in survival curves between groups.

Results

Low expression of DDX58 is associated with a poor prognosis of patients with colon cancer. The activation of DDX58/RIG-I signaling in tumors is a crucial component for checkpoint inhibitor-mediated immunotherapy of cancer (20). In the present study, the association between DDX58 expression and the clinicopathological parameters and prognosis of patients with colon cancer in a tissue microarray was analyzed. The

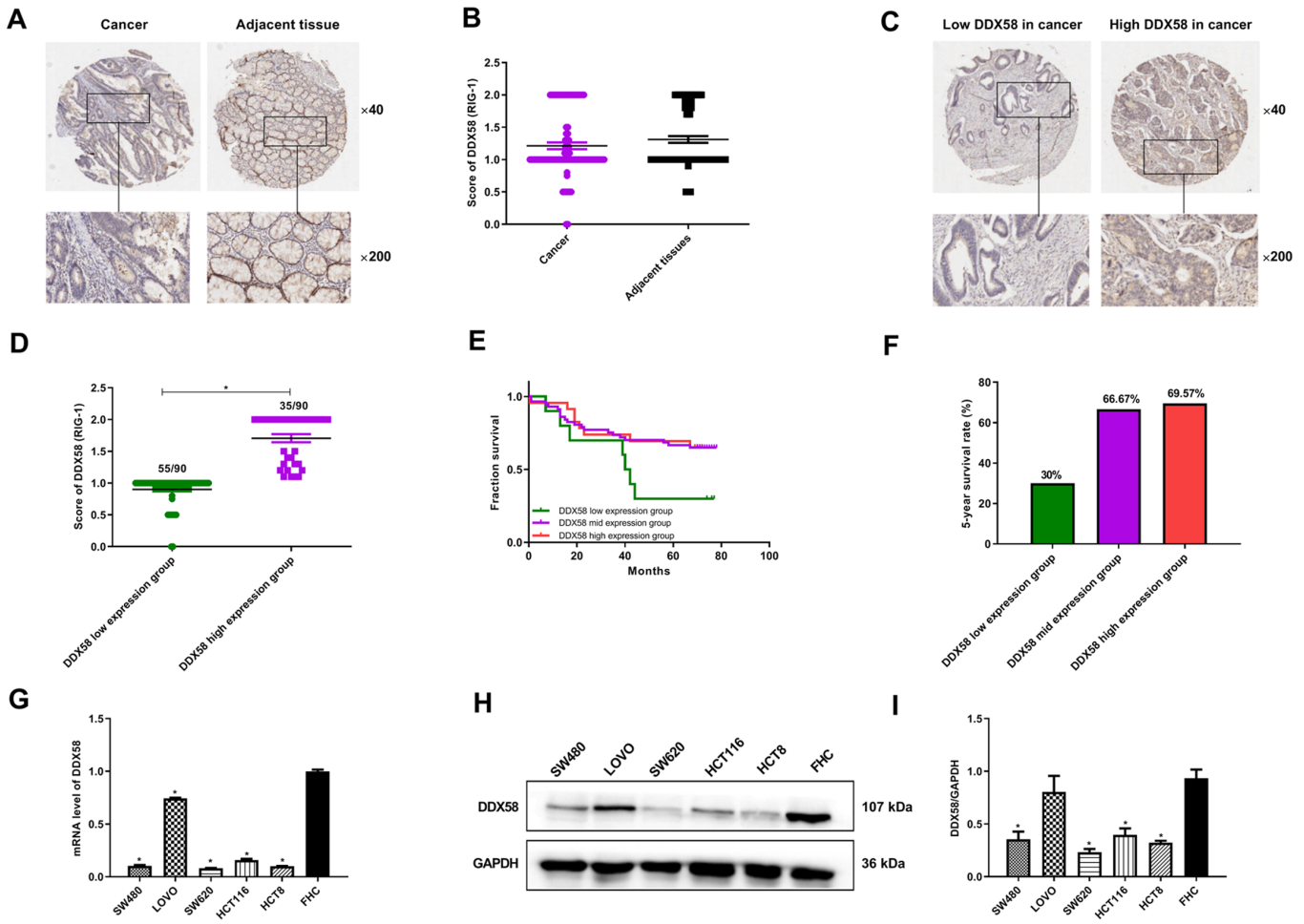

Figure 1. Low expression of DDX58 results in a poor prognosis of patients with colon cancer. (A) Immunohistochemical staining for DDX58 expression in human colon cancer tissues and adjacent tissues. Two representative images are shown. (B) Staining score of DDX58 in human colon cancer tissues and adjacent tissues. Data were analyzed using a paired Student's t-test (P=0.1866). (C) Immunohistochemical staining for DDX58 expression in human colon cancer tissues. Two representative images are shown. (D) Statistical analysis of cases with a low and high expression of DDX58 in human colon cancer tissues. Data were analyzed using an unpaired t-test (*P<0.05). Weakly positive DDX58 staining was considered to represent low protein expression (score ≤1), while positive staining were considered to represent high protein expression (score >1). (E) Association between DDX58 expression and the overall survival of patients with colon cancer. Weak positive DDX58 staining was considered to represent a low protein expression (score <1), a DDX58 staining score ≥1 and <1.5 was considered as medium protein expression, while positive staining was considered to indicate a high protein expression (score ≥1.5). (F) Effect of DDX58 expression on the 5-year survival rate of patients with colon cancer. (G) mRNA level of DDX58 in human colon cancer cell lines. All data are expressed as the mean ± standard deviation. *P<0.05 vs. FHC cells. (H and I) Relative expression of DDX58 protein in human colon cancer cell lines. All data are expressed as the mean ± standard deviation. *P<0.05 vs. FHC cells. SW480, LOVO, SW620, HCT116 and HCT8 were the human colon cancer cell lines. FHC was the human normal colonic epithelial cell line. DDX58, DExD/H-box helicase 58.

results of immunohistochemistry revealed that the level of DDX58 in cancer tissues was slightly lower than that in adjacent tissues, with no statistically significant difference (P=0.1866; Fig. 1A and B). However, it was observed that DDX58 exhibited a low expression in 55 cases and a high expression in 35 cases among the 90 human colon cancer tissues (Fig. 1C and D). It was found that patients with colon cancer with a low expression of DDX58 had a lower 5-year survival rate than patients with a high expression of DDX58 (Fig. 1E and F). However, no notable associations were found between DDX58 expression and patient age or sex, grade, TNM stage and tumor size (data no shown). In addition, RT-qPCR and western blot analysis were performed to detect the mRNA and protein levels of DDX58 in human colon cancer cell lines and lower DDX58 levels were observed in the majority of the colon cancer cell lines compared with FHC normal colon epithelial cells (Fig. 1G-I). These data suggest that a low expression of DDX58 results in a poor prognosis in colon cancer and may represent a potential prognostic biomarker for patients with colon cancer.

Overexpression of DDX58 inhibits the proliferation, migration and invasion of colon cancer cells. In view of the low expression of DDX58 in the majority of the colon cancer cells (while the expression level of DDX58 in LOVO cells was high), and as SW620 and SW480 were derived from the same patient, the classic colon cancer cell lines, HCT8, HCT116 and SW620, were selected for use in subsequent experiments. To evaluate the function of DDX58 in colon cancer cells, a plasmid expressing DDX58 was first used to overexpress DDX58 expression in colon cancer cells and the efficiency of the overexpression system was examined using western blot analysis (Fig. 2A). The results of the MTS and EdU assays revealed that the overexpression of DDX58 distinctly decreased the viability and inhibited the proliferation of the

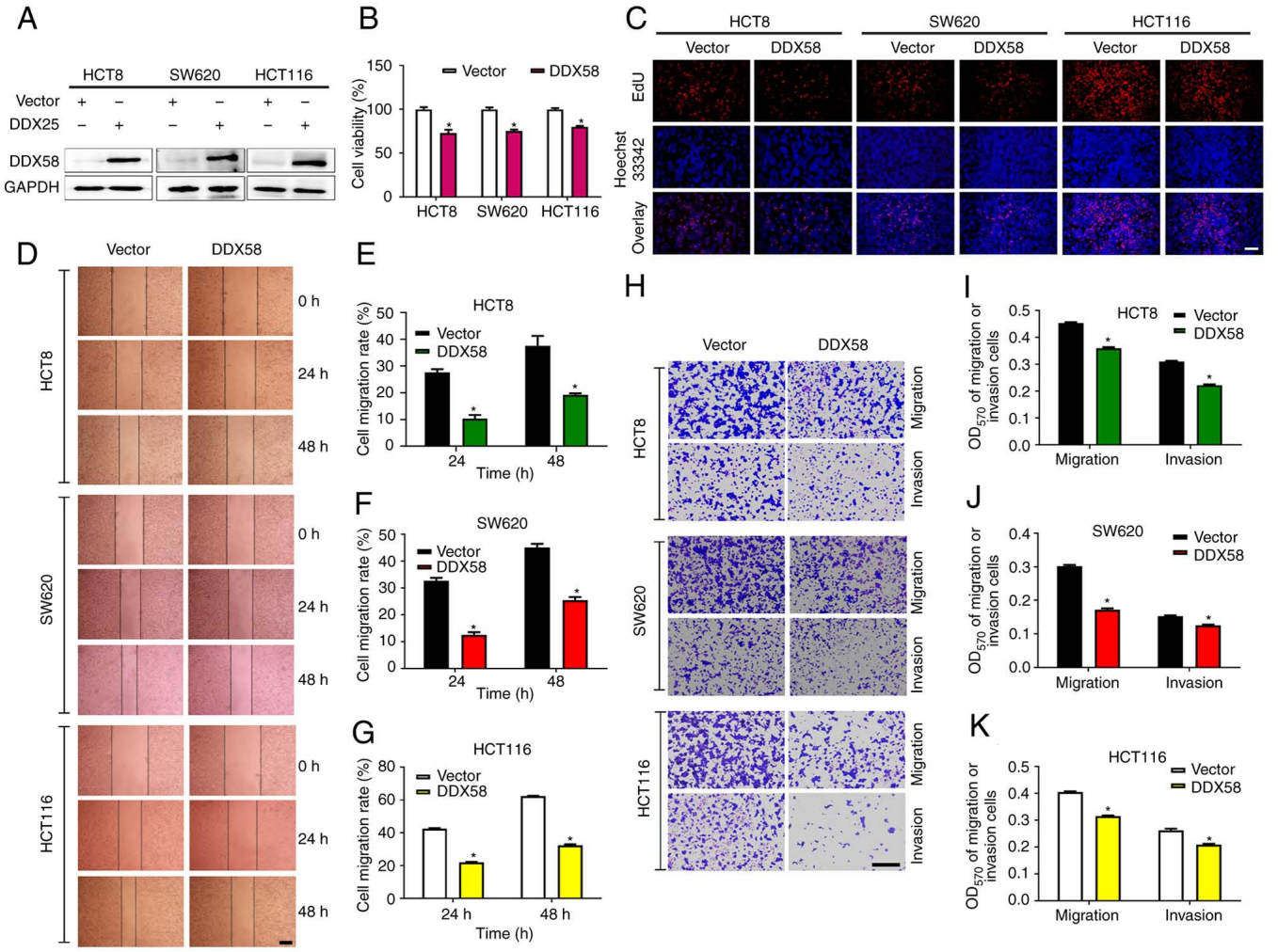

Figure 2. Overexpression of DDX58 inhibits the proliferation, migration and invasion of colon cancer cells. (A) Analysis of the efficiency of DDX58 overexpression in HCT8, HCT116 and SW620 cells. (B and C) Effects of DDX58 overexpression on cell viability and proliferation. Cell viability and cell proliferation were detected using MTS and EdU assays, respectively. Representative images were obtained. Scale bars, 100 μm. (D-G) Wound healing assay was performed to detect the effect of DDX58 upregulation on cell migration. Representative images were obtained. Scale bars, 500 μm. (H-K) Transwell assay was performed to detect the effects of DDX58 upregulation on cell migration and invasion. Representative images were obtained. Scale bars, 200 μm. All data are expressed as the mean ± standard deviation. *P<0.05 vs. the vector group. DDX58, DExD/H-box helicase 58.

HCT8, HCT116 and SW620 cells (Fig. 2B and C). Scratch and Transwell assays also demonstrated that the overexpression of DDX58 significantly inhibited the migration and invasion of HCT8, HCT116 and SW620 cells (Fig. 2D-K). These data thus suggested that the activation of DDX58/RIG-I signaling inhibited the proliferation and metastasis of colon cancer cells.

Silencing of DDX58 promotes the proliferation, migration and invasion of colon cancer cells. To further demonstrate the function of DDX58 in colon cancer cells, specific DDX58 siRNA were used to silence the DDX58 levels in colon cancer cells with the stable overexpression of DDX58 (HCT8/DDX58 and HCT116/DDX58 cells). The results of western blot analysis revealed the efficiency of the silencing of DDX58 (Fig. 3A). Since SW620 cells were constructed as an overexpressing transient cell model, the HCT8/DDX58 and HCT116/DDX58 cells were selected for use to examine the effects of DDX58 silencing on cell viability, proliferation, migration and invasion. The results of MTS, EdU scratch wound and Transwell assays indicated that the downregulation of DDX58 promoted the proliferation, migration and invasion of colon cancer cells with the stable overexpression of DDX58 (Fig. 3B-I), which further demonstrated the function of DDX58 in colon cancer cells.

Overexpression of DDX58 inhibits the expression of CSE in colon cancer cells. CSE, as a major endogenous H_2S synthase, plays critical roles in colon cancer processes, including proliferation, migration and invasion (21-23). In the present study, to further confirm the role of CSE in colon cancer, CSE siRNA was transfected into human colon cancer cells. The results of western blot analysis, and MTS and Transwell assays revealed that CSE was highly expressed in human colon cancer cells (Fig. 4A) and the silencing of CSE expression (Fig. 4B) inhibited the proliferation, migration and invasion of HCT8, HCT116 and SW620 colon cancer cells (Fig. 4C-F). To determine whether DDX58 regulates the progression of colon cancer through CSE, the association between DDX58 and CSE expression in colon cancer cells was first examined and it was found that DDX58 and CSE expression were negatively associated in colon cancer cells (Fig. 4G). Subsequently, DDX58

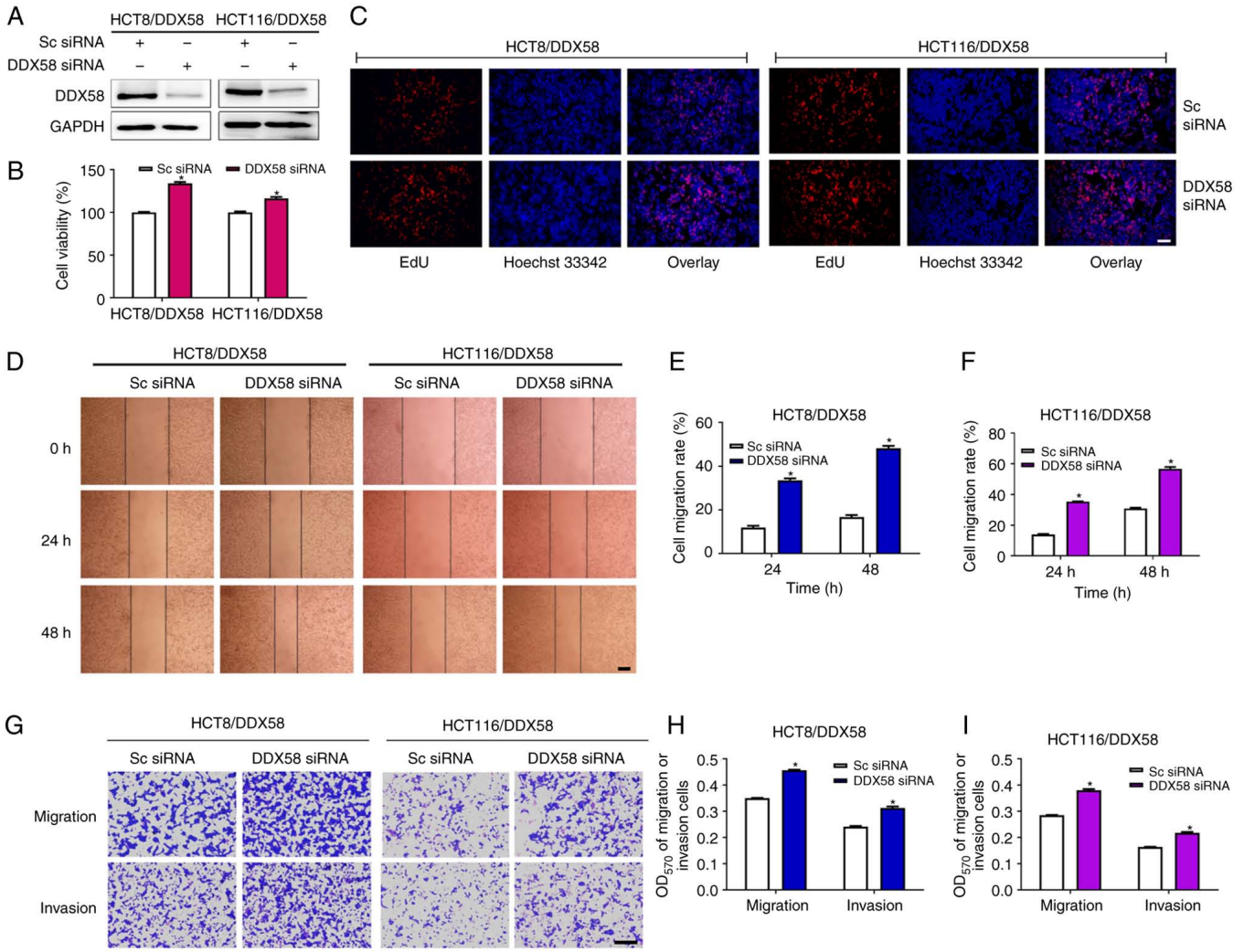

Figure 3. Silencing of DDX58 promotes the proliferation, migration and invasion of colon cancer cells. (A) Analysis of the efficiency of DDX58 knockdown in HCT8/DDX58 and HCT116/DDX58 cells. (B and C) Effects of DDX58 downregulation on cell viability and proliferation. Cell viability and cell proliferation were detected using MTS and EdU assays, respectively. Representative images were obtained. Scale bars, 100 μm. (D-F) Wound healing assay was performed to detect the effect of DDX58 silencing on cell migration. Representative images were obtained. Scale bars, 500 μm. (G-I) Transwell assay was performed to detect the effects of DDX58 silencing on cell migration and invasion. Representative images were obtained. Scale bars, 200 μm. All data are expressed as the mean ± standard deviation. *P<0.05 vs. Sc siRNA group. DDX58, DExD/H-box helicase 58.

overexpression plasmid was transfected into HCT8, HCT116 and SW620 cells, and it was observed that the CSE protein levels were significantly decreased following the overexpression of DDX58 (Fig. 4H and I). Conversely, the silencing of DDX58 led to a significant increase in the CSE protein levels in the HCT-8/DDX58 and HCT116/DDX58 cells with the stable overexpression of DDX58 (Fig. 4H and I). The data demonstrated that DDX58 regulated CSE protein expression in colon cancer cells and indicated that the overexpression of DDX58 suppressed CSE signaling, and consequently inhibited the proliferation, migration and invasion of colon cancer cells.

STAT3 is involved in the regulation of CSE expression in colon cancer cells. In a previous study by the authors, it was demonstrated that STAT3 binds to the promoter of CSE to promote the expression of CSE (24). Therefore, in the present study, to explore the mechanisms underlying altered CSE expression, it was first demonstrated that STAT3 regulates the expression of CSE in colon cancer cells. The HCT8, HCT116 and SW620 cells were transfected with STAT3 siRNA and STAT3 overexpression plasmid. The results of western blot analyses revealed that the silencing of STAT3 suppressed the expression of CSE, while STAT3 overexpression reversed the STAT3 siRNA-induced downregulation of CSE protein levels (Fig. 5), suggesting that STAT3 is involved in the regulation of CSE expression in colon cancer cells. The transfection efficiency of the STAT3 overexpression plasmid in colon cancer cells was also examined (Fig. S1).

DDX58 regulates STAT3 by interacting with STAT3 in colon cancer cells. To explore the role of STAT3 in the regulation of CSE expression by DDX58 in colon cancer cells, the effects of DDX58 on STAT3 expression were first investigated. DDX58 overexpression plasmid was transfected into the HCT8, HCT116 and SW620 cells, and DDX58 siRNA was applied to the HCT8/DDX58 and HCT116/DDX58 cells. Western blot analyses revealed that the overexpression of DDX58 distinctly decreased the level of STAT3, and inhibited the phosphorylation of STAT3

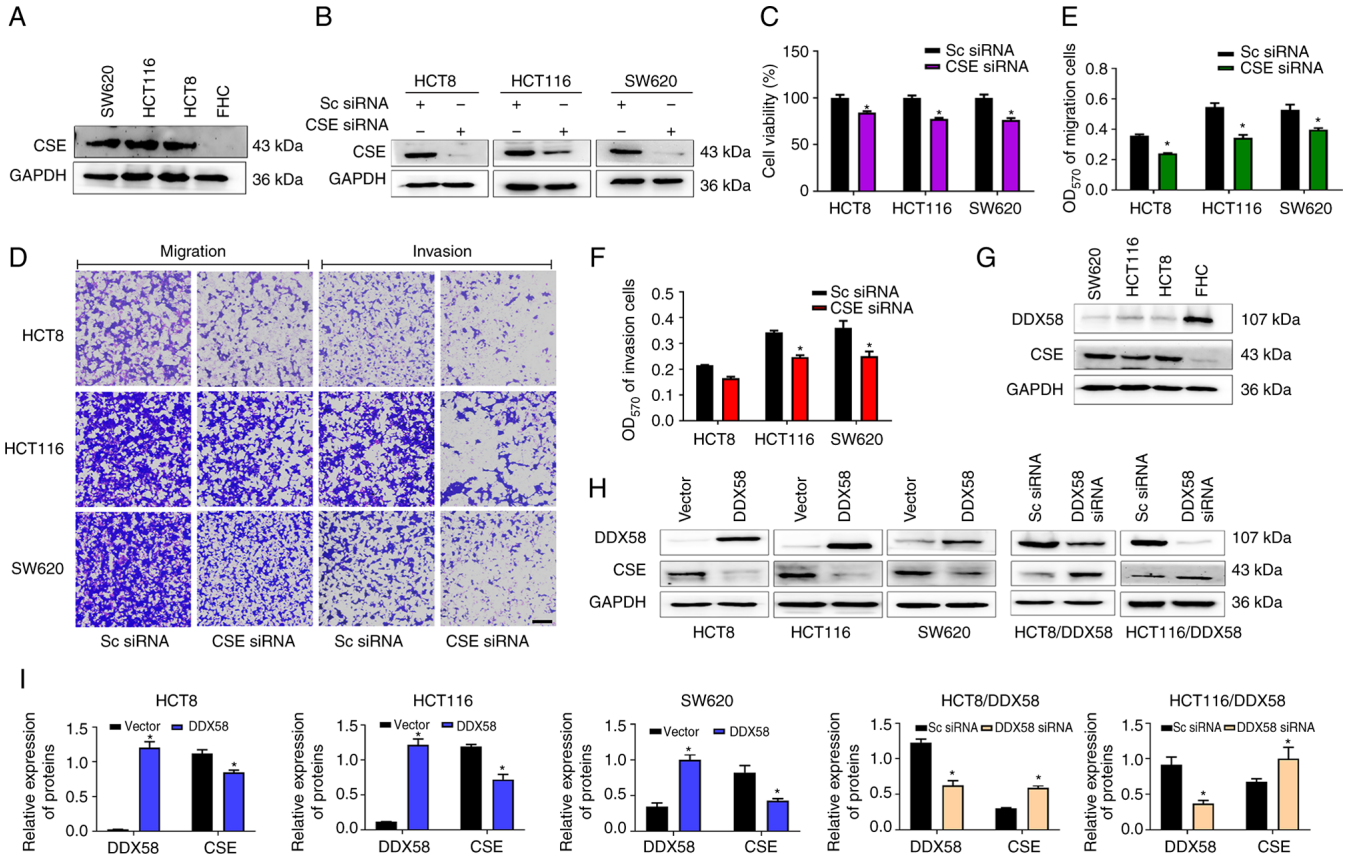

Figure 4. DDX58 affects the expression of CSE in colon cancer cells. (A) CSE is highly expressed in colon cancer cells. (B-F) Effect of CSE knockdown on the survival, migration and invasion of HCT8, HCT116 and SW620 cells. All data are expressed as the mean ± standard deviation. *P<0.05 vs. Sc siRNA group. (G) Association analysis of DDX58 and CSE expression in colon cancer cells. The data demonstrated that DDX58 was negatively associated with CSE expression. (H and I) Effect of the DDX58 level change on CSE expression. The data demonstrated that the CSE protein level was significantly decreased in HCT-8, HCT-116 and SW620 cells following the overexpression of DDX58, while the silencing of DDX58 led to a significant increase in the CSE protein level in HCT-8/DDX58 and HCT116/DDX58 cells. DDX58, DExD/H-box helicase 58.

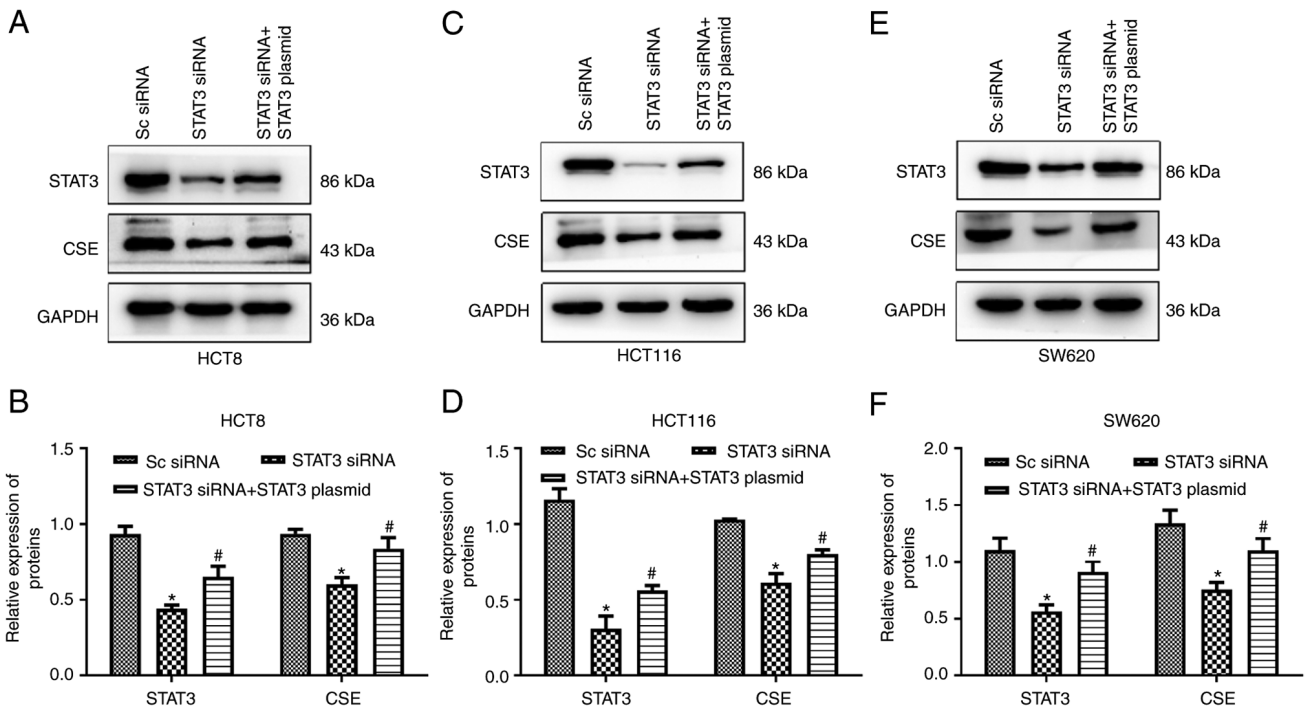

Figure 5. STAT3 regulates the expression of CSE in colon cancer cells. (A and B) Effect of the STAT3 level on CSE protein expression in HCT8 cells. (C and D) Effect of the STAT3 level on CSE protein expression in HCT116 cells. (E and F) Effect of the STAT3 level on CSE protein expression in SW620 cells. All data are expressed as the mean ± standard deviation. *P<0.05 vs. the Sc siRNA group; #P<0.05 vs. the STAT3 siRNA group. CSE, cystathionine-γ-lyase.

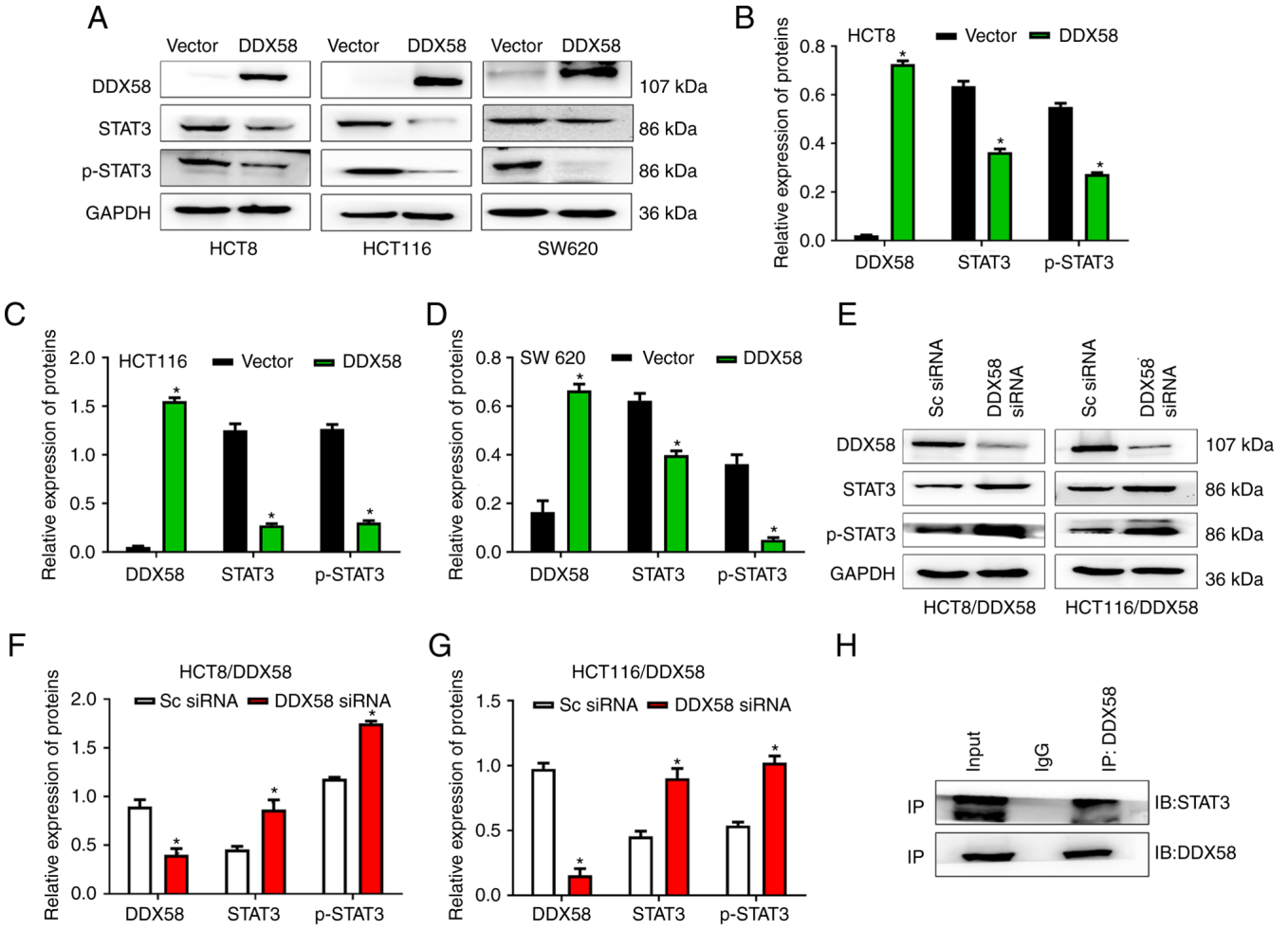

Figure 6. DDX58 regulates the transcriptional activity of STAT3 in colon cancer cells. (A-D) Effect of the overexpression of DDX58 on the levels of STAT3 and pSTAT3 in HCT8, HCT116 and SW620 cells. All data are expressed as the mean ± standard deviation. *P<0.05 vs. the vector group. (E-G) Effect of the silencing of DDX58 on the levels of STAT3 and pSTAT3 in HCT8/DDX58 and HCT116/DDX58 cells. All data are expressed as the mean ± standard deviation. *P<0.05 vs. the Sc siRNA group. (H) DDX58 interacts with STAT3 in colon cancer cells. Overexpression plasmids for DDX58 and STAT3 were co-transfected into human HCT116 cells and co-immunoprecipitation assay was then performed. DExD/H-box helicase 58.

in the HCT8, HCT116 and SW620 cells (Fig. 6A-D); however, the silencing of DDX58 resulted in a significant increase in STAT3 and p-STAT3 levels in the HCT-8/DDX58 and HCT116/DDX58 cells (Fig. 6E-G). These data indicated that DDX58 regulates the expression and phosphorylation of STAT3.

To further explore the mechanisms underlying the effects of DDX58 on STAT3, the interaction between DDX58 and STAT3 was investigated. DDX58 and STAT3 overexpression plasmids were co-transfected into human HCT116 cells and Co-IP assay then was performed. The results revealed that DDX58 interacted with STAT3 in colon cancer cells (Fig. 6H), which may affect the phosphorylation and dimerization of STAT3, and may consequently prevent STAT3 from entering the nucleus, resulting in suppression of the transcription and translation of the target gene, CSE.

Overexpression of DDX58 inhibits tumor growth and STAT3/CSE signaling in a nude mouse xenograft model of colon cancer. To investigate whether DDX58 influences the progression of colon cancer *in vivo*, HCT116 cells with the stable overexpression of DDX58 were injected subcutaneously into the right flanks of nude mice to construct an axillary xenograft tumor model to evaluate the effects of DDX58 on tumor growth. As shown in Fig. 7A-E, the tumors from the mice injected with HCT116 cells with the stable overexpression of DDX58 were smaller in both size and weight, and had a longer tumor doubling time compared with the vector group; this indicated that the overexpression of DDX58 inhibited tumor growth in the nude mouse xenograft model of colon cancer. Moreover, it was found that the levels of STAT3, p-STAT3 and CSE were also decreased in the tumors formed by HCT116/DDX58 cells compared with the vector group (Fig. 7F). The data suggest that the upregulation of DDX58 inhibits tumor growth and STAT3/CSE signaling in a nude mouse xenograft model of colon cancer.

The DDX58 agonist, SB9200, induces the inhibition of human colon cancer. SB9200 (inarigivir soproxil), a dinucleotide antiviral compound, can activate intracellular innate immunity via enabling DDX58/RIG-I. On the basis of the aforementioned results on the function of DDX58 in colon cancer, the present study then investigated the roles of SB9200 in colon cancer cells. Two classic types of colon cancer cells, HCT116 and SW620 cells, were used for subsequent analyses. The data

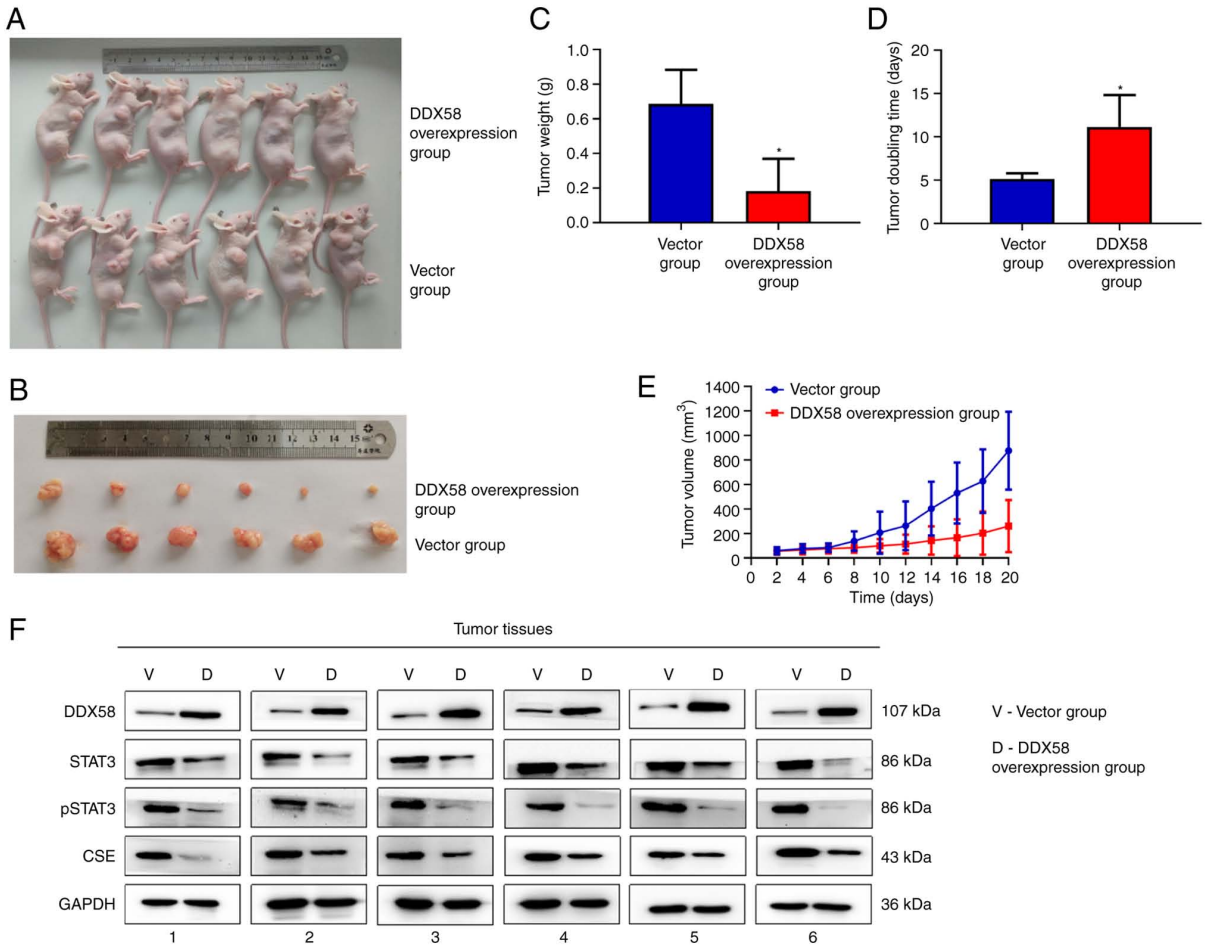

Figure 7. Overexpression of DDX58 inhibits colon cancer growth and downregulates STAT3/CSE signaling *in vivo*. (A-E) HCT116 cells transfected with DDX58 overexpression lentivirus or empty vector lentivirus were respectively injected into the right flanks of BALB/c nude mice and after 3 weeks (A) the mice were sacrificed and (B) the tumors were harvested and (C) weighed; (D) the tumor doubling time was calculated and (E) the volumes of the tumors were recorded. (F) STAT3, p-STAT3 and CSE protein levels in xenograft tumor tissues were assessed using western blot analysis. All data are expressed as the mean ± standard deviation. *P<0.05 vs. the vector group. DExD/H-box helicase 58; CSE, cystathionine-γ-lyase.

demonstrated that SB9200 significantly reduced cell viability and the number of EdU$^+$ cells (Fig. 8A and B), and inhibited the migration and invasion (Fig. 8C-F) of HCT116 and SW620 cells. We also observed an increase in DDX58 protein expression, and a decrease in STAT3, p-STAT3 and CSE expression in HCT116 and SW620 cells treated with SB9200 (Fig. 8G-I). These data indicated that SB9200 induced the inhibition of human colon cancer cells, and further demonstrated the function of DDX58 in colon cancer cells, and the possible use of SB9200 as a therapeutic agent for colon cancer.

The inhibitory effects of DDX58 and its activator, SB9200, on the growth of colon cancer cells by affecting the DDX58/pSTAT3/CSE pathway are summarized in the schematic diagram in Fig. 9.

Discussion

Colon cancer is one of the most common gastrointestinal malignancies and the third most common type of cancer in the United States (25). However, even though the application of chemotherapeutic agents and targeted therapies and the clinical advances in early detection and surgery have been shown to be relatively effective in patients with colon cancer, the 5-year survival rate of patients with metastatic colon cancer remains low (26). Moreover, some patients with colon cancer eventually develop metastasis during treatment (27,28), which most occurs due to the ineffectiveness of standard treatments. Therefore, there is an urgent need for the development of more effective treatment options. Immunotherapy has shown promise in the treatment of colon cancer (20).

DDX58/RIG-I is a natural immune receptor helicase that recognizes double-stranded virus RNA and engages the production of interferons to initiate innate antiviral immunity. Studies have demonstrated that the activation of RIG-I can induce immunogenic cell death in tumor cells (12,29,30), which indicates that it plays a critical role in colon cancer. In the present study, it was found that a low expression of DDX58 resulted in a poor prognosis in colon cancer. It was further confirmed that the overexpression of DDX58 in colon cancer cells attenuated the proliferation, migration and invasion of colon cancer cells *in vitro* and tumor growth *in vivo*, while the opposite was observed following the silencing of DDX58. These data demonstrated the tumor suppressor function of DDX58 in colon cancer. In addition, we observed that the expression level of DDX58 was low in a series of colon cancer cells, while the expression level in LOVO cells was higher than that of other

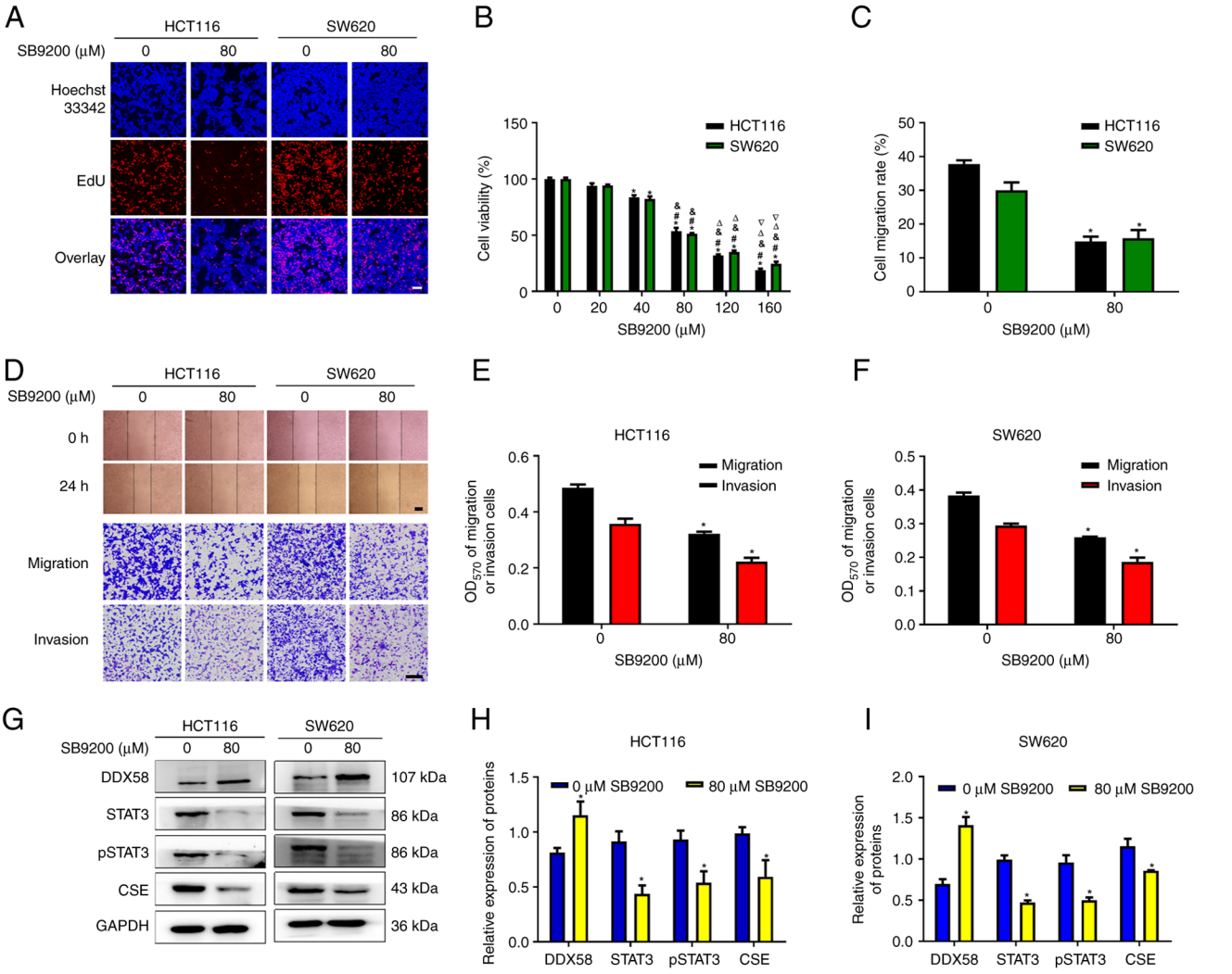

Figure 8. The DDX58 agonist, SB9200, inhibits colon cancer progression. (A and B) Effect of SB9200 on cell proliferation and viability. Cell viability and proliferation were detected using MTS and EdU assays, respectively. Representative images were obtained. Scale bars, 100 μm. *P<0.05 vs. the 0 μM SB9200 group; $^{\#}$P<0.05 vs. the 20 μM SB9200 group; $^{\&}$P<0.05 vs. the 40 μM SB9200 group; $^{\Delta}$P<0.05 vs. the 80 μM SB9200 group. $^{\nabla}$P<0.05 vs. the 120 μM SB9200 group. (C-F) Wound healing and Transwell assays were performed to detect the effects of SB9200 on cell migration and invasion. Representative images were obtained. Scale bars, 500 μm for wound healing assay. Scale bars, 200 μm for Transwell assay. All data are expressed as the mean ± standard deviation. *P<0.05 vs. the 0 μM SB9200 group. (G-I) Effect of SB9200 on the DDX58/pSTAT3/CSE pathway. Western blot analysis was performed to detect the level of DDX58, STAT3, pSTAT3 and CSE proteins. All data are expressed as the mean ± standard deviation. *P<0.05 vs. the 0 μM SB9200 group. DExD/H-box helicase 58; CSE, cystathionine-γ-lyase.

colon cancer cells, which may be related to the characteristics of the cells themselves. For example, LOVO cells were found to proliferate slowly, multiply for a long period of time, and tolerate fewer passages than other cell lines (data not shown).

CSE is a major endogenous H_2S synthase that plays a crucial role in colon cancer (21-23). In the present study, the role of CSE overexpression in promoting colon cancer progression was further confirmed. To identify whether the DDX58 regulation of colon cancer is related to CSE, the association between DDX58 and CSE in colon cancer cells was investigated and the regulatory effects of DDX58 on CSE protein were demonstrated.

STAT3, as a transcriptional mediator of oncogenic signals, is constantly activated in the majority of human cancers (31). An increased pSTAT3 expression has been shown to be inversely associated with the survival of patients with colon cancer (32). Therefore, STAT3 plays a crucial role in the progression of colon cancer. Moreover, a previous study by the authors demonstrated that STAT3 binds to the promoter of CSE to promote the expression of CSE (24). Herein, it was also proven that STAT3 was involved in the regulation of CSE expression in colon cancer cells. Thus, to further explore the underlying mechanisms of the regulation of CSE by DDX58, the effects of DDX58 on the transcriptional activity of STAT3 were determined, and it was found that DDX58 affected the phosphorylation of STAT3 and consequently affected the transcriptional activity of STAT3, which also demonstrated that STAT3 may mediate DDX58 to regulate CSE. In addition, it was also demonstrated that DDX58 interacted with STAT3 in colon cancer cells, and consequently affected the phosphorylation and dimerization of STAT3, resulting in the suppression of the transcription and translation of its target gene, CSE. Furthermore, the inhibitory effect of DDX58 upregulation on STAT3/CSE signaling was also observed in a nude mouse xenograft model of colon cancer.

In addition, it was found that a dinucleotide antiviral compound (SB9200), as a DDX58/RIG-I agonist, induced the inhibition of human colon cancer by affecting the DDX58/

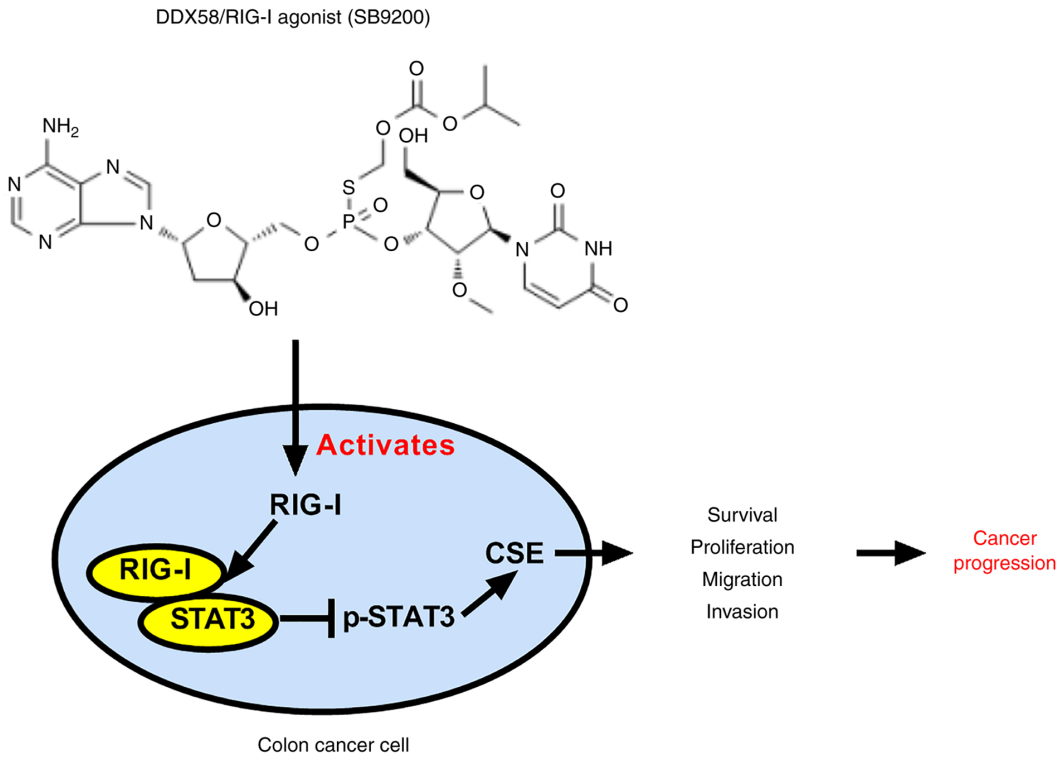

Figure 9. Mechanisms through which the activation of DDX58/RIG-I inhibits the growth of colon cancer cells. DExD/H-box helicase 58; CSE, cystathionine-γ-lyase; RIG-I, retinoic acid-inducible gene-I.

pSTAT3/CSE pathway (Fig. 9), which further demonstrated the tumor suppressive function of DDX58 in colon cancer cells, and the possible use of SB9200 as a therapeutic agent for colon cancer.

In conclusion, the present study revealed a critical tumor suppressor molecule, namely DDX58/RIG-I, in colon cancer. The activation of DDX58/RIG-I inhibited the proliferation of tumor cells by regulating STAT3/CSE signaling in colon cancer. This suggests that the development of DDX58/RIG-I agonists may prove to be a novel and effective therapeutic strategy for patients with colon cancer.

Acknowledgements

Not applicable.

Funding

The present study supported by the grants from the National Natural Science Foundation of China (no. 82072726), as well as the Natural Science Foundation of Henan Province in China (no. 202300410079).

Availability of data and materials

The datasets used and/or analyzed during the current study are available from the corresponding author on reasonable request.

Authors' contributions

TW and KL conceived and designed the experiments. YD, HF and XH performed the experiments. YL, WZ, XZ, CY and WG analyzed the data and produced the figures. YD and TW wrote the manuscript. All authors have read and approved the manuscript and agree to be accountable for all aspects of the research in ensuring that the accuracy or integrity of any part of the work are appropriately investigated and resolved. YD, HF and XH confirm the authenticity of all the raw data.

Ethics approval and consent to participate

All experiments were performed in accordance with national ethical guidelines, all patient consents were obtained and with the approval from the committee of Shanghai Outdo Biotech Co., Ltd. (HCA18ol0Su13). The animal experiments were approved by the Ethics Committee of the Medical School of Henan University (HUSOM2020-301).

Patient consent for publication

Not applicable.

Competing interests

The authors declare that they have no competing interests.

References

1. Kell AM and Gale M Jr: RIG-I in RNA virus recognition. Virology 479-480: 110-121, 2015.
2. Hur S: Double-stranded RNA sensors and modulators in innate immunity. Annu Rev Immunol 37: 349-375, 2019.
3. Streicher F and Jouvenet N: Stimulation of innate immunity by host and viral RNAs. Trends Immunol 40: 1134-1148, 2019.
4. Prasov L, Bohnsack BL, El Husny AS, Tsoi LC, Guan B, Kahlenberg JM, Almeida E, Wang H, Cowen EW, De Jesus AA, *et al*: DDX58(RIG-I)-related disease is associated with tissue-specific interferon pathway activation. J Med Genet 59: 294-304, 2022.

5. Wu S, Lin J, Fu Y and Ou Q: RIG-I enhances interferon-alpha response by promoting antiviral protein expression in patients with chronic hepatitis B. Antivir Ther 23: 575-583, 2018.
6. Loo YM and Gale M Jr: Immune signaling by RIG-Ilike receptors. Immunity 34: 680-692, 2011.
7. Besch R, Poeck H, Hohenauer T, Senft D, Häcker G, Berking C, Hornung V, Endres S, Ruzicka T, Rothenfusser S and Hartmann G: Proapoptotic signaling induced by RIG-I and MDA-5 results in type I interferon-independent apoptosis in human melanoma cells. J Clin Invest 119: 2399-2411, 2009.
8. Duewell P, Steger A, Lohr H, Bourhis H, Hoelz H, Kirchleitner SV, Stieg MR, Grassmann S, Kobold S, Siveke JT, *et al*: RIG-I-like helicases induce immunogenic cell death of pancreatic cancer cells and sensitize tumors toward killing by CD8(+) T cells. Cell Death Differ 21: 1825-1837, 2014.
9. Hou J, Zhou Y, Zheng Y, Fan J, Zhou W, Ng IO, Sun H, Qin L, Qiu S, Lee JM, *et al*: Hepatic RIG-I predicts survival and interferon-alpha therapeutic response in hepatocellular carcinoma. Cancer Cell 25: 49-63, 2014.
10. Xu XX, Wan H, Nie L, Shao T, Xiang LX and Shao JZ: RIG-I: A multifunctional protein beyond a pattern recognition receptor. Protein Cell 9: 246-253, 2018.
11. Elion DL, Jacobson ME, Hicks DJ, Rahman B, Sanchez V, Gonzales-Ericsson PI, Fedorova O, Pyle AM, Wilson JT and Cook RS: Therapeutically active RIG-I agonist induces immunogenic tumor cell killing in breast cancers. Cancer Res 78: 6183-6195, 2018.
12. Jacobson ME, Wang-Bishop L, Becker KW and Wilson JT: Delivery of 5'-triphosphate RNA with endosomolytic nanoparticles potently activates RIG-I to improve cancer immunotherapy. Biomater Sci 7: 547-559, 2019.
13. Ellermeier J, Wei J, Duewell P, Hoves S, Stieg MR, Adunka T, Noerenberg D, Anders HJ, Mayr D, Poeck H, *et al*: Therapeutic efficacy of bifunctional siRNA combining TGF-β1 silencing with RIG-I activation in pancreatic cancer. Cancer Res 73: 1709-1720, 2013.
14. Brägelmann J, Lorenz C, Borchmann S, Nishii K, Wegner J, Meder L, Ostendorp J, Ast DF, Heimsoeth A, Nakasuka T, *et al*: MAPK-pathway inhibition mediates inflammatory reprogramming and sensitizes tumors to targeted activation of innate immunity sensor RIG-I. Nat Commun 12: 5505, 2021.
15. Yang S, Yang C, Yu F, Ding W, Hu Y, Cheng F, Zhang F, Guan B, Wang X, Lu L and Rao J: Endoplasmic reticulum resident oxidase ERO1-Lalpha promotes hepatocellular carcinoma metastasis and angiogenesis through the S1PR1/STAT3/VEGF-A pathway. Cell Death Dis 9: 1105, 2018.
16. Wang L, Shi H, Liu Y, Zhang W, Duan X, Li M, Shi X and Wang T: Cystathionine-γ-lyase promotes the metastasis of breast cancer via the VEGF signaling pathway. Int J Oncol 55: 473-487, 2019.
17. Wang L, Shi H, Zhang XY, Zhang XL, Liu Y, Kang W, Shi X and Wang T: I157172, a novel inhibitor of cystathionine γ-lyase, inhibits growth and migration of breast cancer cells via SIRT1-mediated deacetylation of STAT3. Oncol Rep 41: 427-436, 2019.
18. Nitti M, Piras S, Marinari UM, Moretta L, Pronzato MA and Furfaro AL: HO-1 induction in cancer progression: A matter of cell adaptation. Antioxidants (Basel) 6: 29, 2017.
19. Livak KJ and Schmittgen TD: Analysis of relative gene expression data using real-time quantitative PCR and the 2 (-Delta Delta C(T)) method. Methods 25: 402-408, 2001.
20. Heidegger S, Wintges A, Stritzke F, Bek S, Steiger K, Koenig PA, Göttert S, Engleitner T, Öllinger R, Nedelko T, *et al*: RIG-I activation is critical for responsiveness to checkpoint blockade. Sci Immunol 4: eaau8943, 2019.
21. Fan K, Li N, Qi J, Yin P, Zhao C, Wang L, Li Z and Zha X: Wnt/β-catenin signaling induces the transcription of cystathionine-gamma-lyase, a stimulator of tumor in colon cancer. Cell Signal 26: 2801-2808, 2014.
22. Oláh G, Módis K, Törö G, Hellmich MR, Szczesny B and Szabo C: Role of endogenous and exogenous nitric oxide, carbon monoxide and hydrogen sulfide in HCT116 colon cancer cell proliferation. Biochem Pharmacol 149: 186-204, 2018.
23. Cao X, Ding L, Xie ZZ, Yang Y, Whiteman M, Moore PK and Bian JS: A review of hydrogen sulfide synthesis, metabolism, and measurement: Is modulation of hydrogen sulfide a novel therapeutic for cancer? Antioxid Redox Signal 31: 1-38, 2019.
24. You J, Shi X, Liang H, Ye J, Wang L, Han H, Fang H, Kang W and Wang T: Cystathionine--lyase promotes process of breast cancer in association with STAT3 signaling pathway. Oncotarget 8: 65677-65686, 2017.
25. Siegel R, Desantis C and Jemal A: Colorectal cancer statistics, 2014. Cancer J Clin 64: 104-117, 2014.
26. Lichtenstern CR, Ngu RK, Shalapour S and Karin M: Immunotherapy, inflammation and colorectal cancer. Cells 9: 618, 2020.
27. Vatandoust S, Price TJ and Karapetis CS: Colorectal cancer: Metastases to a single organ. World J Gastroenterol 21: 11767-11776, 2015.
28. Reddy TP, Khan U, Burns EA and Abdelrahim M: Chemotherapy rechallenge in metastatic colon cancer: A case report and literature review. World J Clin Oncol 11: 959-967, 2020.
29. Elion DL and Cook RS: Harnessing RIG-I and intrinsic immunity in the tumor microenvironment for therapeutic cancer treatment. Oncotarget 9: 29007-29017, 2018.
30. Jiang X, Muthusamy V, Fedorova O, Kong Y, Kim DJ, Bosenberg M, Pyle AM and Iwasaki A: Intratumoral delivery of RIG-I agonist SLR14 induces robust antitumor responses. J Exp Med 216: 2854-2868, 2019.
31. Wei N, Li J, Fang C, Chang J, Xirou V, Syrigos NK, Marks BJ, Chu E and Schmitz JC: Targeting colon cancer with the novel STAT3 inhibitor bruceantinol. Oncogene 38: 1676-1687, 2019.
32. Heichler C, Scheibe K, Schmied A, Geppert CI, Schmid B, Wirtz S, Thoma OM, Kramer V, Waldner MJ, Büttner C, *et al*: STAT3 activation through IL-6/IL-11 in cancer-associated fibroblasts promotes colorectal tumour development and correlates with poor prognosis. Gut 69: 1269-1282, 2020.